TOWARDS OPTIMAL RELIEF REPRESENTATION FROM MARS IMAGERY BY COMBINATION OF DEM AND SHAPE-FROM-SHADING

Egon Dorrer[1] and Xiuguang Zhou[2]

[1]) Munich Bundeswehr University, Neubiberg, Germany
[2]) ESRI, Redlands, Cal., USA

ABSTRACT

Described are experimental results of a first approach towards optimal shaded relief representation of the surface of Mars derived from Viking Orbiter digital imagery. The complex problem addresses homogenization and optimization of relief-shading caused by both heterogenious and cartographically improper directions of terrain illumination. The paper deals with the task of removing actual (natural) shading in the original images by a method denoted "de-shading" and subsequent artificial "re-shading" simulating physiologically better illumination direction. Due to space-variant reflectance properties of the physical surface, occurrences of shadows, and mostly non-existence of a high quality digital terrain model, the mathematical problem is, in principle, ill-posed and requires certain regularity and smoothness conditions for the derivation of reasonable solutions. Shape-from-shading (SFS) methods alone can provide relative shape information only for surfaces with constant albedo and, at least, two different illumination directions. Since this is unrealistic for planetary surfaces, an integral estimation approach utilizing even low quality DEM's generated by stereo photogrammetry may lead to better solutions. In the paper a modified iterative SFS-algorithm originally published by Zheng and Chellappa is described by using the simple Lambert photometric model. For the first time, space-variant albedo could be estimated by means of a special region growing algorithm. Experimental results for a Viking orbiter image of Mars, for which no height information was available, and for a Clementine orbiter Lunar image with a fairly smooth digital elevation model given, are discussed. They indicate the principal possibility of recovering albedo as well as improving the DEM; however, also the deficiencies of the method become apparent.

1   INTRODUCTION

Interpretation and analyses of remotely sensed imagery or topographic image maps derived therefrom are seriously hampered if the terrain illuminating direction significantly deviates from the upper left as seen by the observer. The reason for this well known physiological and psychological phenomenon stems from the observation that image shading induced by "wrong" illumination – i.e. if above criterion is not met – may give rise to spatially reverse impressions of the imaged terrain relief. This effect is apparent in the portion of a Viking image of Mars in the upper part of Fig. 1 where light comes from the bottom (angular deviation 135°). Contrary to that, the lower part of Fig. 1 – here simply the negative of the upper picture simulating illumination from the top – yields proper, i.e. upright, relief impression (angular deviation 45°).

One of the sub-tasks within a photogrammetry-cartography working group of the scientific program of the unsuccessful international Mars '96 mission was an attempt to process Mars imagery – to be acquired by a German-made high resolution three-line stereo camera (HRSC) developed at DLR in Berlin – in order to both optimize and homogenize relief-shading for proper, hence immediate depth perception in larger map areas. Here, homogenization is understood as image mosaicking in order to have identical illumination conditions, whereas optimization means generating best possible depth perception.

Although still within the theoretical and experimental investigation level, we nevertheless have come up with some important intermediate results that are to be dis-

cussed in the sequel. The paper deals with the problem of removing the actual (natural) shading situation in the original images by a method denoted "de-shading" and subsequent artificial "re-shading" simulating more appropriate illumination directions.

Reverse ("wrong") depth perception

Proper depth perception

Figure 1. Perception of terrain relief depending on direction of illumination

The complexity of the entire problem asks for an integrated approach, i.e. a combination of photogrammetry (shape-from-stereo) with photoclinometry (shape-from-

D. Fritsch, M. Englich & M. Sester, eds, 'IAPRS', Vol. 32/4, ISPRS Commission IV Symposium on GIS - Between Visions and Applications, Stuttgart, Germany.

Dorrer & Zhou 157

shading). On the one hand, the mostly featureless Martian surface, unsuited for precise digital image matching necessary for three-dimensional surface reconstruction, may provide qualitatively good slope information via shading to be used for "intelligent" interpolation into photogrammetric information. On the other hand, sharp topographic edges, i.e. slope discontinuities, can substantially improve, again by their shading information, the basically smoothing image matching results. It is to be expected that such an integrated approach will enable the separation of space-variant albedo.

2 METHOD OF DE-SHADING

Since appropriate surface reflectance characteristics are virtually unknown due to generally varying physical surface material properties as well as occurrences of umbrae on steep slopes and cast shadows, de-shading must be considered a rather complex task. Without proper knowledge of a high resolution DEM, in principle the problem is ill-posed and requires certain regularity and smoothness conditions for the derivation of somewhat reasonable solutions. Only very special cases. e.g. constant surface albedo and simple reflectance function, may yield more or less acceptable solutions without DEM information. In this case, relative surface slopes may be fully or partially recovered from shading information on images. There is extensive literature in the field of photoclinometry where so-called "Shape-from-shading" methods have been and are being developed. However, very little has been done in order to combine shape-from-shading with available DEM information. It can be shown that, e.g. low quality DEMs may be somewhat improved if SFS-methods are employed, although varying surface albedo gives rise to height and brightness artifacts.

A first viable solution presented in (Zhou et al., 1996) has been successively modified and improved. Fig. 2 shows a simplified diagram of the current version that can cope only with the simple Lambert photometric model, i.e. complete diffuse reflection. The inputs to the process are the original or already oriented (e.g. orthorectified) brighta brightness image, the direction of illumination, and a digital elevation model (DEM) or elevation image. The latter may be substituted for by the two terrain gradient images derived from the DEM. The terrain data first permits removal of all shadow areas from the shading-relevant areas. Space-variant albedo, i.e. image intensity not caused by shading, is estimated at each point by means of a region growing algorithm. The elevation gradients are then adjusted according to a variational problem by minimizing the difference between original intensity image and computed reflectance map subject to certain constraints (see below). The method employed stems from a modified global shape-from-shading approach common in photoclinometry (see e.g. Kirk, 1987). The improved elevation gradients are then used to compute improved estimates of the reflectance map through re-shading. The whole process involves an iteration strategy.

In the sequel, the four sub-processes within the iteration loop in Fig. 2 are discussed in more detail.

2.1 Localization of shadow areas

Shadow areas, both umbrae and cast shadows, must be investigated separately, as their reflectance properties are completely different from sunlit areas. Umbrae are shad-

ows on steep surface slopes unreachable by direct sun light, thus possessing rather low intensity levels. Cast shadows are caused by other objects obscuring the light source. Their reflectance properties are mainly characterized by ambient light sources. Considering the overall complexity of the photometry of shadows, in our present version we merely filtered out the shadow areas from the image data by means of a ray-tracing method applied to the DEM data. It is anticipated to solve the problem from a theoretical viewpoint in a later version. Currently, the shadows are merely filled in by region growing. The developed preliminary ray-tracing program tool may also be used to determining the illumination direction.
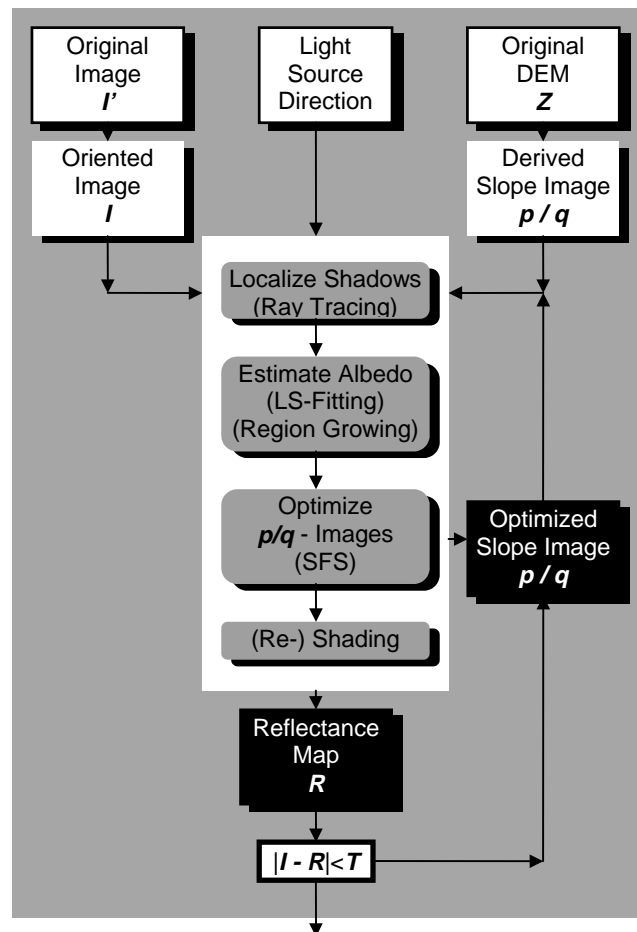
Figure 2. Modelling of Lambert surface reflectance

2.2 Estimation of pixel-based albedo

Space variant albedo is estimated by a special region growing algorithm. Albedo values are first assigned individually to each pixel according to

$$A(x,y) = \frac{\bar{I}(x,y)}{R(p(x,y),q(x,y))}$$

where $\bar{I}$ is the intensity of the original image smoothed to the resolution level of the given Z-map (DEM), and R is the Lambert reflectance map derived from $Z(x,y)$ and the known light source direction.

D. Fritsch, M. Englich & M. Sester, eds, 'IAPRS', Vol. 32/4, ISPRS Commission IV Symposium on GIS - Between Visions and Applications, Stuttgart, Germany.

158   IAPRS, Vol. 32, Part 4 "GIS-Between Visions and Applications", Stuttgart, 1998

Assuming a seeding kernel $\omega - 1$ of constant albedo $A_{\omega-1}$ found through the homogeneity criterion

$$\sigma^2(A_{\omega-1}) < T_0 ,$$

with a reasonably chosen starting threshold value T_0 to be estimated from the whole image area, a new kernel ω results from adding a neighbor pixel if the error measure

$$e_\omega^2 = \sum_{x,y \in \omega}[\bar{I}(x,y) - A_\omega \cdot R(x,y)]^2$$

is smaller than a suitably determined and to the growing kernel dynamically adapted, threshold value T. The albedo of "left-over" pixels is estimated by linear interpolation into the "grown" pixels. The new albedo is then determined by the least squares relation

$$A_\omega = \frac{\sum_\omega \bar{I} \cdot R}{\sum_\omega R^2} .$$

2.3   SFS for Improvement of DEM

We mainly followed an algorithm published by Zheng & Chellappa (1991), except for an analytical rather than numerical determination of the partial derivatives of the reflectance function. In addition to the intensity gradient and range (here: elevation) gradient constraints there, we have incorporated as third constraint the integrability condition, considering it crucial for the solution of the SFS problem. In fact, our results became acceptable only after including this constraint.

The solution of the SFS problem constitutes a constrained variational problem, i.e. the functions $p(x,y)$ and $q(x,y)$ representing the surface slopes with respect to the coordinates x, y, and $Z(x,y)$ representing the DEM as elevation image, are to be optimally adjusted in order to minimize the functional

$$\iint F(x,y;p,q,p_x,p_y,q_x,q_y;Z,Z_x,Z_y,Z_{xy})dx\,dy = \text{min.}$$

The function F to be integrated is defined by the compound expression

$$\begin{aligned} F = \ & [I(x,y) - R(p(x,y),q(x,y))]^2 \\ & + \lambda\,[(I_x - R_x)^2 + (I_y - R_y)^2] \\ & + \mu\,[(Z_x - p)^2 + (Z_y - q)^2] \\ & + \nu\,[(Z_{xy} - p_y)^2 + (Z_{xy} - q_x)^2] \end{aligned}$$

where λ, μ, ν represent the Langrange multipliers according to three constraints, viz. intensity gradient constraint, surface slope constraint, and integrability constraint, the latter being another form of the condition $p_y = q_x$. The associated Euler equations are given by the partial differential equations

$$F_p - \frac{\partial}{\partial x}F_{p_x} - \frac{\partial}{\partial y}F_{p_y} = 0$$

$$F_q - \frac{\partial}{\partial x}F_{q_x} - \frac{\partial}{\partial y}F_{q_y} = 0$$

$$F_Z - \frac{\partial}{\partial x}F_{Z_x} - \frac{\partial}{\partial y}F_{Z_y} + \frac{\partial^2}{\partial x\partial y}F_{Z_{xy}} = 0$$

and yield as solution optimal estimates for the functions p, q ("p/q-images") and Z subject to the employed constraints. In the present version the Lagrange multipliers are treated as variables rather than functions and, for reasons of simplicity, a priori values are assigned to them. This will have to be improved in a later version.

2.4   (Re-) Shading

Shading may principally be considered a relatively simple and straight forward cartographic task, as the nature of the photometric model is virtually immaterial. Therefore, the reflectance properties of the shaded surface are usually taken as of Lambert-type. A somewhat comprehensive and terrain-adaptive algorithm has been published in Zhou et al. (1995). Application of the shading algorithm to the optimized p- and q-images results in a reflectance image R that should approximate the original brightness image I. Only if the absolute image difference $\left|\bar{I} - R\right|$ has smaller values than a properly chosen threshold image T, can the entire process be considered finished. Besides R and the optimized p-/q-images, the albedo A and an optimized DEM will be obtained. The whole process has to be repeated iteratively until convergence towards T has been achieved.

2.5   Application of Wavelet Transform

As has been published elsewhere (see, e.g., Zhou et al., 1995; 1997), two-dimensional Haar wavelet transforms may be favorably utilized for fast computation of partial derivatives. In our approach, therefore, all partial derivative images, i.e. intensity gradients and elevation gradients, needed for the numerical solution of the Euler equations, are determined in this way.

In principle, wavelets are families of functions

$$H^{a,b}(x) = \frac{1}{\sqrt{a}}H\!\left(\frac{x-b}{a}\right),\ a,b \in R, a \neq 0$$

where H is the Haar mother wavelet, a and b are scaling and shifting parameters, respectively. An image is decomposed into four sub-bands giving rise to a wavelet representation pyramid structure with three detail images and one approximation image depending on the decomposition level. The partial derivatives follow immediately from the detail images.

3   EXPERIMENTAL RESULTS

Preliminary tests of our developed de-shading system were carried out with two extreme scenes, viz. one small area on the Moon with available DEM information but with highly varying surface albedo, the other on Mars without height information but with assumed constant albedo.
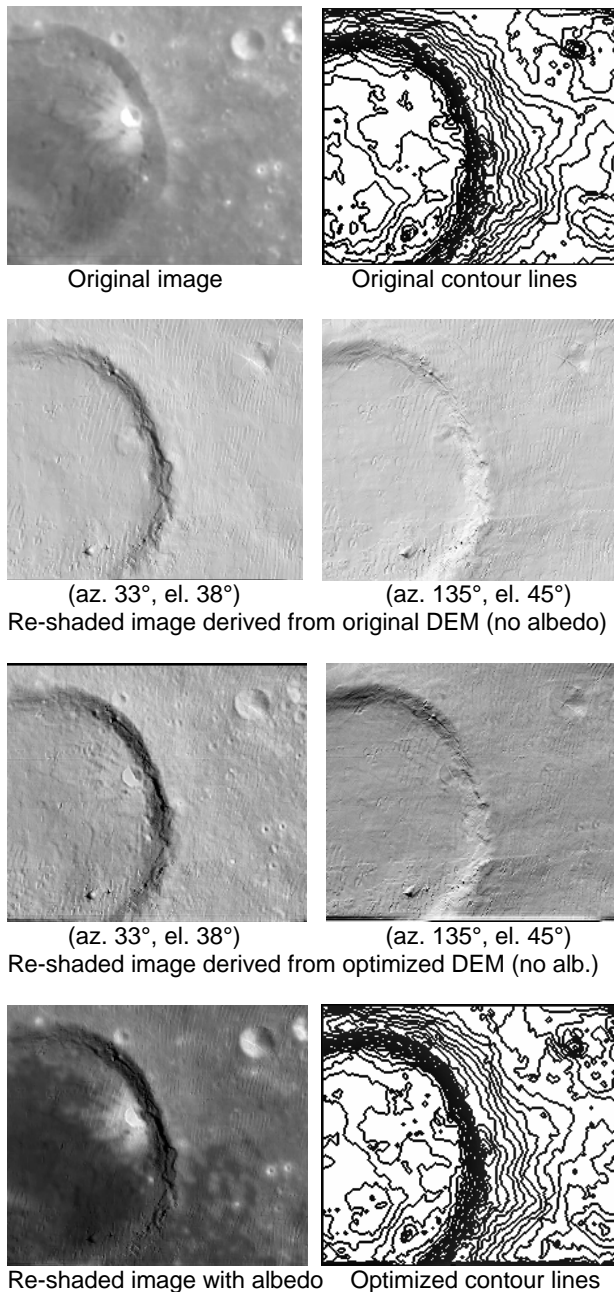
D. Fritsch, M. Englich & M. Sester, eds, 'IAPRS', Vol. 32/4, ISPRS Commission IV Symposium on GIS - Between Visions and Applications, Stuttgart, Germany.

Dorrer & Zhou   159

Original image   Original contour lines

(az. 33°, el. 38°)   (az. 135°, el. 45°)
Re-shaded image derived from original DEM (no albedo)

(az. 33°, el. 38°)   (az. 135°, el. 45°)
Re-shaded image derived from optimized DEM (no alb.)

Re-shaded image with albedo   Optimized contour lines

Figure 3. SFS/DEM experiment with Clementine orbiter
                 Lunar imagery

3.1   Clementine Lunar Imagery

Fig. 3 exhibits a series of different images of a relatively small lunar scene taken by the orbiting satellite Clementine. A DEM of this scene, obtained through digital image correlation techniques, was provided by DLR in Berlin. The DEM contains substantial deficiencies as can be easily seen from the contour lines that were derived from the DEM. Notice, e.g., that the small bright crater within the large crater is not visible from the contours, neither are the two small craters in the upper right part of the scene. This fact is enhanced in the two shaded relief images in the second row which were directly derived from the original DEM. An additional gross error appears as a small but steep peak in the lower part of the crater. Shading in the picture on the left corresponds to the original

illumination direction from the upper right (azimuth is counted counter clockwise from east). In the picture on the right a cartographically pleasing light source direction from the upper left has been assumed for shading.

The efficiency of the described new method manifests itself in the two pictures in the third row. Obviously the shape-from-shading part has contributed to a noticeable improvement of the original DEM. This is true, however, only with shading obtained from illumination directions close to the original light source (picture on the left). Shape-from-shading fails practically completely for an illumination direction that is approximately perpendicular to the original (picture on the right). In other words, no improvement of the DEM may be expected orthogonally to the original light source direction if the DEM, as in this example, does not contain sufficiently resolved correct detail height information.

The picture on the left in the fourth row represents the re-shaded scene with estimation of the albedo. Comparison with the original image in the first row indicates rather good agreement, thus proving the capability of the chosen solution.

3.2   Viking Mars Imagery

Fig. 4 exhibits a Viking Orbiter image of an area North of the Ius Chasma, part of the Western Valles Marineris on Mars. Approximate location is 7° South latitude and 83° West longitude. South is on the top of the picture. The scene is only partially mapped on the Topographic Image Map published by Neugebauer et al. (1997).


Figure 4. Original Viking Orbiter image
(South is on the top)

The area covers a flat mesa (altitude 7500 m) with a large ancient crater of some 22 km diameter, and is eroded by a deep tributary valley of Ius Chasma. The lowest point lies about 5000 m below the mesa level. Illumination is exactly from the bottom of the image causing a typical effect of relief reversal. The albedo on the mesa surface was assumed to be constant, although some portions in the bottom part of the image appear to be darker due to different surface material. Inspite of that, the scene has been considered appropriate for a test of the developed method

D. Fritsch, M. Englich & M. Sester, eds, 'IAPRS', Vol. 32/4, ISPRS Commission IV Symposium on GIS - Between Visions and Applications, Stuttgart, Germany.

160   IAPRS, Vol. 32, Part 4 "GIS-Between Visions and Applications", Stuttgart, 1998

assuming height information not being available.

The two pictures shown in Fig. 5 are brightness representations of the final optimized partial derivatives of a relative $Z(x,y)$, i.e. p-image as x-derivative and q-image as y-derivative, as a result of the described algorithm. All original Z-values were assumed to be zero. Therefore, the algorithm must purely rely on shape-from-shading and cannot discriminate albedo from shading. As the original horizontal light source direction is parallel to the y-axis (North-South), only the y-derivative can be determined sufficiently reliable (q-image on the right). The x-derivative (East-West), on the contrary, is indeterminate.
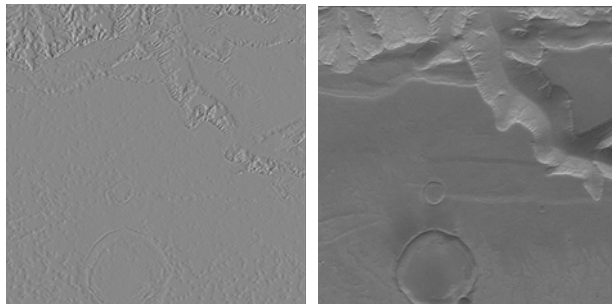
p-image   q-image
Figure 5. Slope images after shape-from-shading
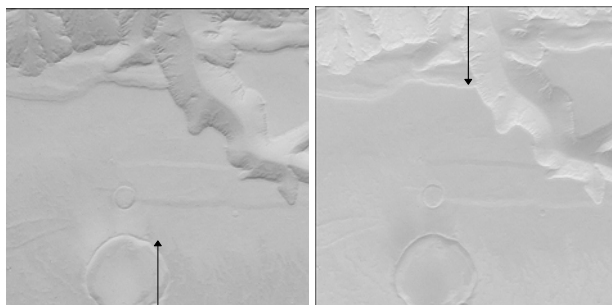
Re-shaded with original   Re-shaded with opposite
light source direction   light source direction
Figure 6. Re-shaded images

Finally, Fig. 7 illustrates re-shading with four different illumination directions, the upper left one coming closest to optimal relief perception.

 It is anticipated to carry out further investigations on Viking Orbiter Mars imagery by using existing digital elevation models.

4   CONCLUSIONS

The results so far clearly show the feasibility of the developed algorithm for manipulating image shading according to different light source directions. Also, shape-from-shading with simple Lambert reflection may be favorably utilized in conjunction with digital elevation models in order to estimate space-variant albedo and improve the given elevations. Apparent deficiencies still contained in the present version of the algorithm will have to be investigated further. In this way, main emphasis must be placed on the inclusion of high resolution DEM's, combination of shape-from-shading with shape-from-stereo, incorporation

of different image geometry according to existing camera types, integration of shadow areas, and studies of different reflectance models.

The reflectance image R as optimal estimate of I and main result of the entire algorithm is shown in the left hand picture of Fig. 6. It compares favorably with the original image of Fig. 4, despite the different brightness level. The picture on the right of Fig. 6 was obtained by re-shading from the opposite direction, demonstrating correct depth perception of the relief.
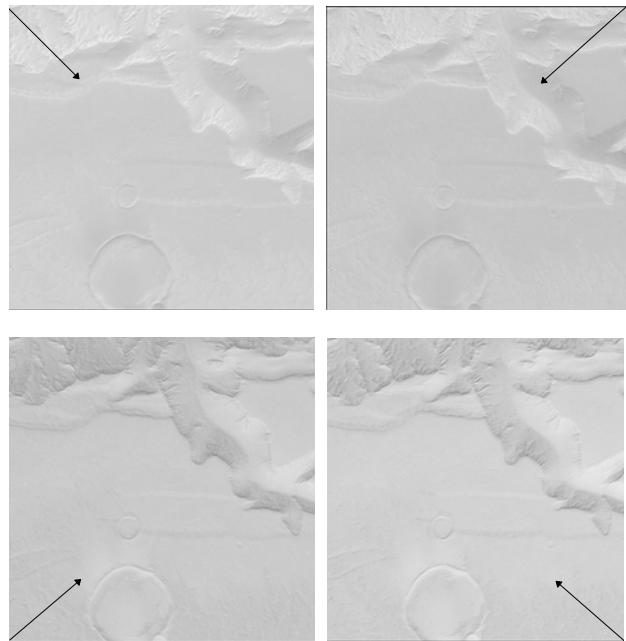

Figure 7. Re-shaded scene from four different directions

REFERENCES

Dorrer, E., **X. Zhou** (1997): De- and Re-Shading for optimal relief mapping of the surface of Mars. In: L. Ottoson (ed.): Proceedings 18th ICA/ACI International Cartographic Conference ICC 97, Gävle 1997, Vol. 2, 1150-1158.

Kirk, R. L. (1987): A Fast Finite-Element Algorithm for Two-Dimensional Photoclinometry. Part III of Ph.D. Thesis, Division of Geological and Planetary Sciences, California Institute of Technology, Pasadena.

Neugebauer, G., E. Dorrer, X. Zhou (1997): Prototype of a Topographic Image Map 1:500000 of Mars (in German). Kartographische Nachrichten, 47(1997)5, 167-173; with a map sheet.

D. Fritsch, M. Englich & M. Sester, eds, 'IAPRS', Vol. 32/4, ISPRS Commission IV Symposium on GIS - Between Visions and Applications, Stuttgart, Germany.

Dorrer & Zhou   161

Zheng, Q, R. Chellappa (1991): Estimation of illumi-
nant direction, albedo and shape from shading. IEEE
Trans. On PAMI, 13(7)pp. 680-702.

Zhou, X., **E. Dorrer** (1995): An adaptive algorithm of
shaded-relief images from DEMs based on wavelet
transform. In: E. A. Fedosov (ed.): Digital Photogram-
metry and Remote Sensing. SPIE Proceedings Series,
Vol. 2646, 212-224

Zhou, X., **E. Dorrer** (1996): De-Shading: Integrated
approach to photometric model, surface shape and
reflectance properties. Int. Arch. Phot. & Rem. Sensing,
Vol. XXX!, Part B3, Vienna 1996, 1028-1035

Zhou, X, E. Dorrer (1997): A New Edge Detection
Algorithm Based on Wavelet Transform. In: Altan -
Gründig (Eds): Second Turkish-German Joint Geodetic
Days, Berlin, 1997, 727-736.